Geochemistry Geophysics Geosystems G3
AN ELECTRONIC JOURNAL OF THE EARTH SCIENCES
Published by AGU and the Geochemical Society

Article
Volume 9, Number 2
12 February 2008
Q02007, doi:10.1029/2007GC001766
ISSN: 1525-2027

New constraints on the Pb and Nd isotopic evolution of NE Atlantic water masses

S. B. Muiños
Instituto Nacional de Engenharia, Tecnologia e Inovação, Departamento de Geologia Marinha, Estrada da Portela, Apartado 7586, P-2721-866, Alfragide, Portugal (susana.muinos@ineti.pt)

Leibniz Institute for Marine Sciences, IFM-GEOMAR, Wischhofstrasse, 1-3, D-24148 Kiel, Germany (smuinos@ifm-gcomar.de)

M. Frank
Institute for Isotope Geology and Mineral Resources, Department of Earth Sciences, ETH Zurich, Zurich, Switzerland

Now at Leibniz Institute for Marine Sciences, IFM-GEOMAR, Wischhofstrasse, 1-3, D-24148 Kiel, Germany

C. Maden
Institute for Particle Physics, ETH Zurich, Zurich, Switzerland

Now at Institute for Isotope Geology and Mineral Resources, Department of Earth Sciences, ETH Zurich, NW C 83.1, Clausiusstrasse 25, CH-8092 Zurich, Switzerland

J. R. Hein
U.S. Geological Survey, 345 Middlefield Road, MS 999, Menlo Park, California 94024, USA

T. van de Flierdt
Institute for Isotope Geology and Mineral Resources, Department of Earth Sciences, ETH Zurich, Zurich, Switzerland

Now at Lamont Doherty Earth Observatory and Department of Earth and Environmental Sciences, Columbia University, 61 Route 9W, Palisades, New York 10964, USA

S. M. Lebreiro, L. Gaspar, and J. H. Monteiro
Instituto Nacional de Engenharia, Tecnologia e Inovação, Departamento de Geologia Marinha, Estrada da Portela, Apartado 7586, P-2721-866, Alfragide, Portugal

A. N. Halliday
Institute for Isotope Geology and Mineral Resources, Department of Earth Sciences, ETH Zurich, Zurich, Switzerland

Now at Department of Earth Sciences, University of Oxford, Parks Road, Oxford OX1 3PR, UK

[1] Time series of lead (Pb) and neodymium (Nd) isotope compositions were measured on three ferromanganese crusts recording the evolution of NE Atlantic water masses over the past 15 Ma. The crusts are distributed along a depth profile (~700–4600 m) comprising the present-day depths of Mediterranean Outflow Water and North East Atlantic Deep Water. A pronounced increase of the $^{206}Pb/^{204}Pb$ in the two deeper crusts starting at ~4 Ma and a decrease in $^{143}Nd/^{144}Nd$ in all three crusts took place between ~6–4 Ma and the present. These patterns are similar to isotope time series in the western North Atlantic basin and are consistent with efficient mixing between the two basins. However, the

changes occurred 1–3 Ma earlier in the eastern basin indicating that the northeastern Atlantic led the major change in Pb and Nd isotope composition, probably due to a direct supply of Labrador Seawater via a northern route. The Pb isotope evolution during the Pliocene-Pleistocene can generally be explained by mixing between two end-members corresponding to Mediterranean Outflow Water and North East Atlantic Deep Water, but external sources such as Saharan dust are likely to have played a role as well. The Pb isotope composition of the shallowest crust that grew within the present-day Mediterranean Outflow Water does not show significant Pb isotope changes indicating that it was controlled by the same Pb sources throughout the past 15 Ma.

Components: 11,037 words, 6 figures, 4 tables.

Keywords: ferromanganese crusts; radiogenic isotopes; seawater chemistry; northeastern Atlantic; Mediterranean Outflow Water; North East Atlantic Deep Water.

Index Terms: 1040 Geochemistry: Radiogenic isotope geochemistry; 1050 Geochemistry: Marine geochemistry (4835, 4845, 4850); 4835 Oceanography: Biological and Chemical: Marine inorganic chemistry (1050).

Received 25 July 2007; **Revised** 24 October 2007; **Accepted** 7 November 2007; **Published** 12 February 2008.

Muiños, S. B., M. Frank, C. Maden, J. R. Hein, T. van de Flierdt, S. M. Lebreiro, L. Gaspar, J. H. Monteiro, and A. N. Halliday (2008), New constraints on the Pb and Nd isotopic evolution of NE Atlantic water masses, *Geochem. Geophys. Geosyst.*, *9*, Q02007, doi:10.1029/2007GC001766.

1. Introduction

[2] The strength of the present-day Meridional Overturning Circulation, which controls deep ventilation and meridional heat transport around the globe, has to a large extent been controlled by the strength of North Atlantic Deep Water (NADW) production. Three principal water masses contribute to the formation of NADW at high northern latitudes: Labrador Seawater (LSW), Denmark Strait Overflow Water (DSOW), and Iceland-Scotland Overflow Water (ISOW), to which variable amounts of Subpolar Mode Water are admixed [*Schmitz and McCartney*, 1993]. In addition, it has been suggested that contributions of highly saline and warm Mediterranean Outflow Water (MOW) are important for the salt and temperature budget of the North Atlantic, thereby preconditioning water masses that form NADW [cf. *Reid*, 1978; *Voelker et al.*, 2006]. In the western north Atlantic, NADW flows south within the Western Boundary Undercurrent and reaches the eastern North Atlantic basin through gaps in the Mid-Atlantic Ridge such as the Romanche or Vema fracture zones [cf. *Broecker et al.*, 1985]. North East Atlantic Deep Water (NEADW) is formed by mixing of a branch of ISOW, which did not flow into the Northwestern basin, with LSW, Lower Deep Water (LDW, which is essentially modified Antarctic Bottom Water (AABW)) and modified NADW [*Lacan and Jeandel*, 2005a].

[3] NADW production and export to the Southern Ocean have been subject to temporal changes but the magnitude and timing of those changes has been a matter of debate. It has been argued that NADW export was not fully established until the closure of the Isthmus of Panama (beginning at around 12.5 Ma and final closure at ~3 Ma [*Murdock et al.*, 1997, and references therein]). According to this hypothesis the closure caused an enhanced advection of warm and saline waters to the northern high latitudes which then increased the production of NADW [*Bartoli et al.*, 2005]. In contrast, there are clear indications from carbon and neodymium isotope studies that the NADW export was stronger during the warm early Pliocene than it is today [*Ravelo and Andreasen*, 2000] and decreased after the major intensification of Northern Hemisphere Glaciation (NHG) at 2.7 Ma [*Raymo et al.*, 1992; *Frank et al.*, 2002]. Moreover, based on Nd isotope records from the Walvis Ridge, *Via and Thomas* [2006] postulated an onset of NADW production in the early Oligocene, in agreement with sedimentological evidence [*Davies et al.*, 2001].

[4] Another important factor that probably influenced thermohaline circulation during the Miocene was the Messinian Salinity Crisis (MSC). During the MSC between 5.96 and 5.33 Ma [*Krijgsman et al.*, 1999], the Mediterranean was, at least periodically, isolated from the global ocean, which led to the deposition of large evaporate sequences. By the end of the MSC, the exchange of water between

the Mediterranean Sea and the Atlantic was reestablished and highly saline and warm MOW entered the North Atlantic through the Strait of Gibraltar. Present MOW properties show the existence of two cores of this water mass: an upper core, centered at about 800 m, and a lower core, at 1200 m water depth [*Madelain*, 1970; *Zenk*, 1970; *Ambar and Howe*, 1979; *Ambar et al.*, 1999, 2002]. The changes during the Miocene MSC and the interruption of MOW inflow into the North Atlantic most likely had a profound impact on overturning circulation and Northern Hemisphere climate [*Johnson*, 1997; *Rogerson et al.*, 2006].

[5] In order to better understand long-term changes of ocean circulation and weathering inputs into the ocean on a million-year timescale, the radiogenic isotope compositions of Pb and Nd have been used as proxies. These elements have residence times on the order of or shorter than the global mixing time of the ocean and can therefore be used as proxies for water mass mixing [cf. *Frank*, 2002]. Radiogenic isotopes are not influenced by biological fractionation processes, and change their values only as a function of water mass mixing or by additions from external sources such as riverine, aeolian, or in the case of Pb, hydrothermal inputs [cf. *Frank*, 2002; *van de Flierdt et al.*, 2004]. In addition, exchange processes at the boundaries of the oceans such as shelf areas (termed boundary exchange) may alter the Nd isotopic composition of seawater [*Lacan and Jeandel*, 2005b] and submarine groundwater discharge may also play a role in controlling the dissolved Nd isotope signature of seawater [*Johannesson and Burdige*, 2007].

[6] The present-day Nd isotope composition of water masses, as measured directly on seawater samples, shows that the most radiogenic isotope compositions are found in the North Pacific, whereas the least radiogenic values are found in the North Atlantic, generally reflecting the isotopic composition of the rocks surrounding the main ocean basins [cf. *Frank*, 2002]. Newly formed NADW has an ε_{Nd} signature of -13.5 [*Piegras and Wasserburg*, 1982, 1987; *Jeandel*, 1993; *Lacan and Jeandel*, 2005a] (Nd isotope ratios are expressed as ε_{Nd} values; This notation refers to the deviation of the measured $^{143}Nd/^{144}Nd$ ratio from the chondritic uniform reservoir CHUR, which value is 0.512638, multiplied by 10,000). The unradiogenic Nd isotope signature of NADW today mainly originates from the LSW component. This water mass today has a very unradiogenic signature ($\varepsilon_{Nd} = -13.9 \pm 0.4$) [*Lacan and Jeandel*, 2005a] caused by weathering contributions from old Archean rocks which in the Baffin Bay area reach an ε_{Nd} as low as -26 [*Stordal and Wasserburg*, 1986]. In comparison, DSOW ($\varepsilon_{Nd} = -8.4 \pm 1.4$) and ISOW ($\varepsilon_{Nd} = -8.2 \pm 0.6$) have much more radiogenic signatures [*Piegras and Wasserburg*, 1987; *Lacan and Jeandel*, 2005a]. In the Northeastern Atlantic, NEADW has an Nd isotopic signature of -13.2 ± 0.4 [*Lacan and Jeandel*, 2005a] whereas modified NEADW show less negative ε_{Nd} values varying between -11.3 and -11.9 [*Tachikawa et al.*, 1999; *van de Flierdt et al.*, 2006]. At shallower depth (0–1100 m), Nd isotope ratios of the seawater in the northeastern Atlantic show more negative values (ε_{Nd} down to -13) probably due to the contribution by partial dissolution of Saharan dust particles (Saharan dust has ε_{Nd} values between -12 and -14) [e.g., *Grousset et al.*, 1988; *Tachikawa et al.*, 1997]. For deeper waters (below 2500 m) the dissolved Nd isotope signature can be explained by mixing between NADW and AABW [e.g., *Frank et al.*, 2003]. Southern Ocean waters, such as AABW and Antarctic Intermediate Water, have less radiogenic ε_{Nd} values (-7 to -9) [*Piegras and Wasserburg*, 1982; *Bertram and Elderfield*, 1993; *Jeandel*, 1993] as a result of the contribution of Pacific waters with higher ε_{Nd} values (-3 to -5) reflecting weathering of young volcanic rocks [*Piegras and Jacobsen*, 1988].

[7] The preanthropogenic Pb isotope distribution in deep waters, which cannot be measured on seawater, has been recovered from ferromanganese crust surfaces [*Abouchami and Goldstein*, 1995; *von Blanckenburg et al.*, 1996a] and shows that the most radiogenic compositions are found in the NW Atlantic ($^{206}Pb/^{204}Pb > 19.1$) whereas less radiogenic values prevail in the Southern Ocean ($^{206}Pb/^{204}Pb < 18.9$) and in the central North Pacific (e.g., $^{206}Pb/^{204}Pb < 18.7$). The highly radiogenic Pb isotope values in the North Atlantic have been explained by incongruent weathering processes on the old cratonic landmasses of northern Canada and Greenland [*von Blanckenburg and Nägler*, 2001].

[8] Changes in radiogenic isotope signatures recorded in fish teeth [e.g., *Thomas*, 2004; *Martin and Scher*, 2004; *Scher and Martin*, 2006; *Thomas and Via*, 2007] or planktonic foraminifera [*Vance and Burton*, 1999; *Vance et al.*, 2004] deposited in marine sediments, or in ferromanganese crusts (hereafter called crusts) have been used as proxies [cf. *Frank*, 2002]. Crusts are seawater precipitates

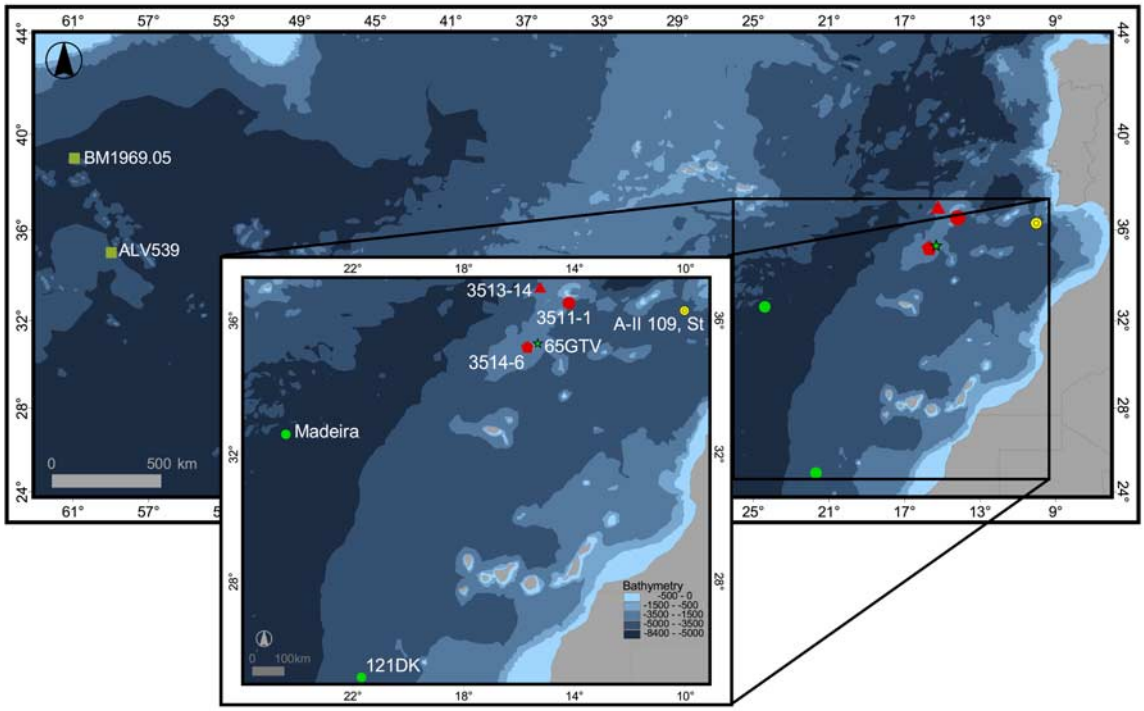

Figure 1. Map showing the location of the three studied crusts (in red) plus 65GTV (green star) from a nearby location [*Abouchami et al.*, 1999]. Data from 121DK [*Abouchami et al.*, 1999] and Madeira [*Reynolds et al.*, 1999] (green circles), and the A-II 109, St. 95 ε_{Nd} profile [*Piegras and Wasserburg*, 1983] (yellow circle) from the NE Atlantic as well as crusts BM1969.05 and ALV539 [*Burton et al.*, 1997, 1999; *Reynolds et al.*, 1999] (dark green squares) from the NW Atlantic were also applied in our study (bathymetry from Gebco).

which grow at very slow rates (about 0.5–10 mm/Ma) and recorded the radiogenic isotope evolution of seawater as far back as 75 Ma [*Klemm et al.*, 2005]. Several time series studies based on ferromanganese crust time series in the western North Atlantic have shown that the ε_{Nd} of NADW has decreased significantly over the past 3 Ma [*Burton et al.*, 1997, 1999; *O'Nions et al.*, 1998]. This was either caused by increased weathering contributions from old cratonic areas in northern Canada and Greenland or by an increased admixture of LSW. In the eastern North Atlantic similar patterns have been observed, though with a smaller amplitude [*Abouchami et al.*, 1999; *Reynolds et al.*, 1999]. A contribution from LSW entering via a northern route [*Sy et al.*, 1997; *Paillet et al.*, 1998; *Abouchami et al.*, 1999; *Bower et al.*, 2002; *Frank et al.*, 2003] has been suggested to have occurred in the eastern basin. In addition, MOW contributions ($\varepsilon_{Nd} = -9.4 \pm 0.3$ [*Spivack and Wasserburg*, 1988; *Abouchami et al.*, 1999; *Tachikawa et al.*, 2004]) have clearly played a role for the radiogenic isotope composition of the water masses in the eastern basin, particularly at shallow depths.

[9] We present new high-resolution and high-precision Pb and Nd isotope time series obtained from three crusts in the eastern North Atlantic Ocean. These data provide a 15 Ma isotopic history of water masses at different depths in the eastern North Atlantic, which varied as a function of changes in ocean circulation and weathering inputs.

2. Material and Methods

[10] Three hydrogenous crusts covering water depths between ~700 and 4600 m in the eastern North Atlantic Ocean were analyzed for Pb and Nd isotopes, bulk element chemistry, and mineralogy. The samples were collected during Meteor Cruise 51/1 (2001) [*Hoernle and Scientific Party*, 2003] (Figure 1 and Table 1) between the Portuguese southwest coast and Madeira Island. Crusts 3514-6 (Lion seamount) and 3511-1 (Josephine seamount) were collected east of the Madeira-Tore Rise, whereas crust 3513-14 was collected on the western flank of the Rise. The crusts were sampled continuously in steps of 0.5 mm for the top first centimeter of the crust and in steps of 1 mm for the remaining depths. Sampling was performed per-

Table 1. Locations and Details of Three Crusts From Meteor Cruise M51/1[a]

Sample	Name Used in Text	Location	Latitude, °N	Longitude, °W	Water Depth, m	Thickness,[b] mm	Growth Rates, mm/Ma	Base Age, Ma
417DR-6Mn	3514-6	Lion seamount, cone at SW margin	35° 12.7–13.0	15° 42.03–42.36	938–688	**23.5**		15.2
						0–9.5	1.37	
						9.5–17	2.45	
						17–23.5	1.25	
410DR-1Mn	3511-1	Josephine seamount, southern flank	36° 30.5–30.7	14° 12.48–13.04	2436–2161	**18**		12.0
						0–10.5	1.25	
						10.5–18	2.04	
414DR-14Mn	3513-14	Madeira-Tore Rise, NW margin	36° 58.2	15°44.90–44.80	4586–4603	**43**		11.4
						0–5	1.76	
						5–43	4.45	

[a] The coordinates and depth ranges correspond to the "on" and "off" of the bottom data from each dredge station.
[b] The total thickness of the sample is given in bold; the depth intervals correspond to each depth interval with a different growth rate.

pendicular to the macroscopic growth laminations using a computer-controlled drill with 10 mm diameter. The methods used for chemical preparation and purification of Nd and Pb were adopted from *Cohen et al.* [1988] and *Galer and O'Nions* [1989], respectively. Nd and Pb isotope ratios were determined by MC-ICP-MS (Nu Instruments) at ETH Zürich. For the Pb isotope measurements, a Tl-doping procedure [e.g., *Belshaw et al.*, 1998] was applied. The $^{143}Nd/^{144}Nd$ ratio was normalized to $^{146}Nd/^{144}Nd = 0.7219$ for instrumental mass bias correction. Age-corrected $\varepsilon_{Nd(T)}$ values were calculated using $^{147}Sm/^{144}Nd = 0.115$. Errors shown on the figures correspond to $2\sigma_{(SD)}$ external reproducibilities, obtained by repeated measurements of standard materials. All isotope ratios presented were normalized to standard values: JMC-Nd, with a $^{143}Nd/^{144}Nd$ ratio of 0.511833 cross-calibrated to the La Jolla standard (0.511858) was used. For the NIST SRM981 Pb standard the ratios used for external normalization are those given by *Abouchami et al.* [1999]. For the Nd isotope measurements of different sessions, the 2σ external precision varied between 30 ppm and 33 ppm, whereas for Pb isotope measurements the 2σ external precision was 116, 144, 172, 46, and 74 ppm for $^{206}Pb/^{204}Pb$, $^{207}Pb/^{204}Pb$, $^{208}Pb/^{204}Pb$, $^{207}Pb/^{206}Pb$, and $^{208}Pb/^{206}Pb$, respectively. In-run precision for each sample was better than the external reproducibility. The crusts were dated using $^{10}Be/^{9}Be$ profiling applying a 1.51 Ma half-life of ^{10}Be [*Hofmann et al.*, 1987]. The ^{10}Be data were measured at the AMS facility of ETH Zürich and Paul Scherrer Institute, Switzerland. The samples were measured applying a newly developed carrier-free method, in which the natural $^{10}Be/^{9}Be$ ratios were determined directly [*Maden et al.*, 2004] (Table 2). The reduced accuracies of the older $^{10}Be/^{9}Be$ ratios were caused by the low ion currents extracted from the samples.

[11] The samples were analyzed for bulk element chemistry by ICP-MS/AES at the National Oceanography Centre, Southampton, U.K. The chemical preparation of the samples included a first dissolution step in 6M HCl and a second dissolution step of the residue in hydrofluoric and perchloric acids, which were combined for the elemental analyses, of which only the Mn, Fe and Co concentrations are used in this study. Internal rock standards and blanks were used to calibrate the data. X-ray diffraction analyses (for 3511-1 and 3514-6) were conducted on a Philips diffractometer, using Cu-Kα radiation and a carbon curved-crystal monochromator, at the United States Geological Survey. These analyses showed that the Fe-Mn oxyhydroxide fraction of the samples throughout consists of δMnO_2 (vernadite), the main mineral in crusts of hydrogenetic origin. The mineralogy, taken together with the Mn/Fe ratios (0.58 to 1.26) and the growth rates (see section 3) confirm an entirely hydrogenetic origin and allows the crusts to be used as reliable archives of paleoceanographic events [*Koschinsky et al.*, 1996; *Hein et al.*, 2000].

3. Results

3.1. Dating

[12] Growth rates obtained from the $^{10}Be/^{9}Be$ profiles vary between 1.3 and 4.5 mm/Ma (Figure 2 and Tables 1 and 2), which is in the range expected

Table 2. The $^{10}Be/^{9}Be$ Dating and Growth Rates

Depth, mm	Error, mm	$^{10}Be/^{9}Be$, $\times 10^{-9}$	Absolute Error, $\times 10^{-9}$	Relative Error, %	Growth Rates, mm/Ma	Ages, Ma	Error 2σ[a]	Linear Ages	Co, W %
				3514-6					
0.00								0.00	0.585
0.50	0.50	26.96	1.97	7.30		0.48	±0.04	0.36	0.758
4.25	0.75	5.16	0.49	9.47	1.03	4.11	±0.39	3.10	0.565
9.50	1.00	1.33	0.28	20.96	1.77	7.08	±1.48	6.93	0.467
				3511-1					
0.00								0.00	0.565
3.00	0.50	20.86	2.27	10.90		2.78	±0.30	2.40	0.729
5.75	0.75	6.54	0.75	11.46	1.08	5.32	±0.61	4.60	1.026
10.25	0.75	1.78	0.31	17.26	1.58	8.17	±1.41	8.20	0.735
				3513-14					
0.00								0.00	0.760
5.00	0.50	13.71	1.05	7.65		1.05	±0.08	1.12	0.554
9.25	0.75	9.14	1.15	12.54	4.78	1.93	±0.24	2.08	0.268
18.50	0.50	4.20	0.39	9.32	5.42	3.64	±0.34	4.16	0.185
26.75	0.75	1.42	0.34	23.81	3.47	6.02	±1.43	6.01	0.142

[a] The σ values correspond to standard error of the mean (SEM).

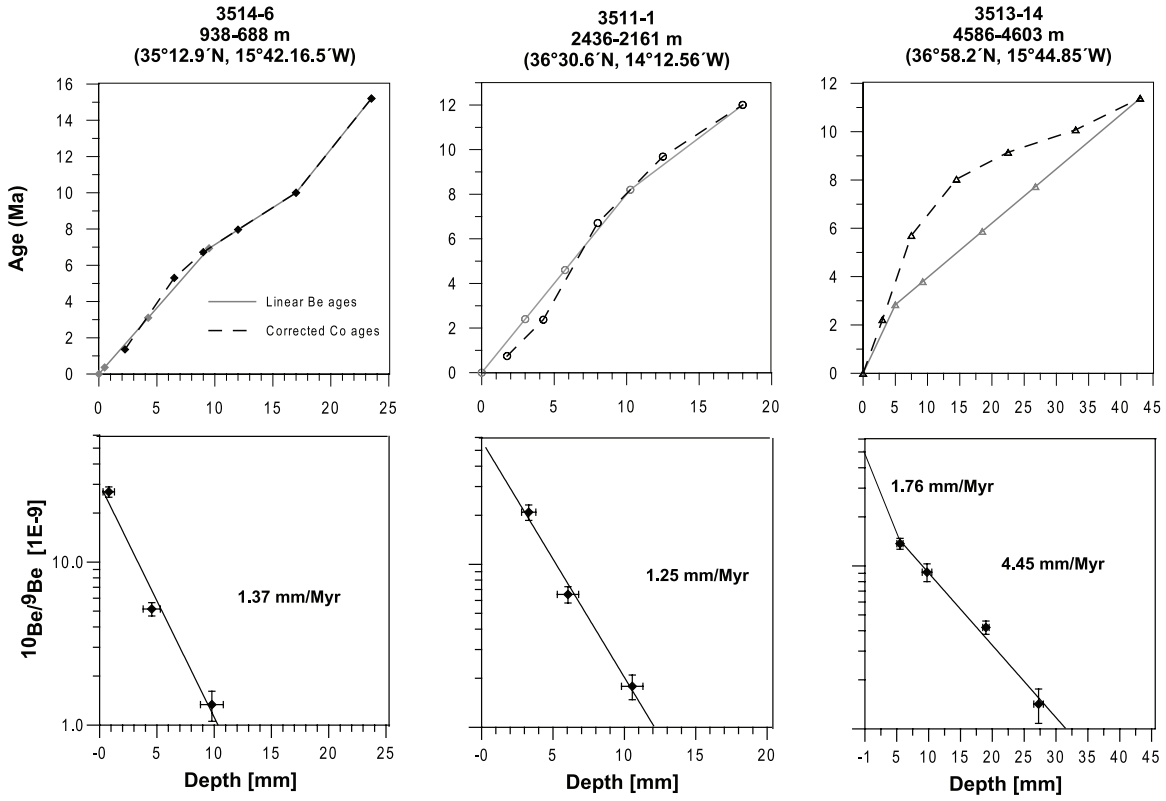

Figure 2. Profiles of $^{10}Be/^{9}Be$ ratios for the three crusts studied versus depth. The ages of the applied age models given by the solid lines in the age versus depth plots were calculated with a half-life for ^{10}Be of 1.5 Ma. The growth rates and ages beyond the age range covered by $^{10}Be/^{9}Be$ data were determined using the Co constant flux method [*Manheim*, 1986; *Frank et al.*, 1999a] and were rectified to match the $^{10}Be/^{9}Be$-derived growth rate in the upper part of the two shallower crusts, respectively (dashed line).

for hydrogenetic ferromanganese crusts [e.g., *Hein et al.*, 2000; *Frank*, 2002]. Intermediate depth crust 3511-1 has an extrapolated surface $^{10}Be/^{9}Be$ ratio of $\sim 5 \times 10^{-8}$, which corresponds to values expected for modern seawater precipitates in the eastern North Atlantic Ocean [*von Blanckenburg et al.*, 1996b]. The shallowest crust 3514-6 has a lower surface $^{10}Be/^{9}Be$ ratio of 2.7×10^{-8} and also deepest crust 3513-14 has a lower extrapolated surface $^{10}Be/^{9}Be$ ratio of 2.3×10^{-8}. The lower $^{10}Be/^{9}Be$ value in the shallowest crust is consistent with water column data from similar water depths in the northwestern Atlantic [*Ku et al.*, 1990] and with admixture of waters from the Mediterranean (the location of the crust is presently bathed by MOW), which have very low $^{10}Be/^{9}Be$ ratios of $\sim 1 \times 10^{-8}$ [*Brown et al.*, 1992]. Alternatively, if the true actual surface $^{10}Be/^{9}Be$ ratio of all crusts were 5×10^{-8}, this would imply that a layer representing ~1.5 Ma of crust growth (~2 mm) is missing from the surface of shallowest crust 3514-6. Given that there are no macroscopically visible hints for erosion or dissolution at the surface of this crust, we consider this highly unlikely. For following interpretations we will therefore consider the $^{10}Be/^{9}Be$ ratio of 2.7×10^{-8} as the correct surface value, but will briefly discuss the implications of a possibly missing surface layer in section 4.5. For deepest crust 3513-14 the low $^{10}Be/^{9}Be$ ratio may either imply that there is a thick layer representing 1.5 Ma of crust growth missing (~6.6 mm) or that the crust grew much more slowly at about 1.7 mm/Ma in the uppermost 5 mm, where we have no $^{10}Be/^{9}Be$ data. Such a lower growth rate is fully consistent with the growth rate variability derived from the Co constant flux method [*Manheim*, 1986; *Frank et al.*, 1999a] which was consequently adopted for the applied age model in the upper 5 mm (Figure 2). The oldest part of the crusts 3514-6 and 3511-1 was not dated by $^{10}Be/^{9}Be$ but growth rates were determined by matching the Co constant flux method in each crust to $^{10}Be/^{9}Be$ in their respective younger part [*Manheim*, 1986; *Frank et al.*, 1999a]. The results of the Co method indicate that the average growth rates obtained from $^{10}Be/^{9}Be$ in the younger parts of crusts 3514-6 and 3511-1 were not significantly different from their older parts. The dating resulted in ages of 15.2 Ma, and 12.0 Ma for the bases of the crusts at 23.5 mm and 18 mm depth of crusts 3514-6 and 3511-1, respectively. For deep crust 3513-14, the Co-derived growth rate did not match the well-constrained $^{10}Be/^{9}Be$ growth rate, but indicates relatively constant growth below 5 mm, which is why the age model for this crust is only based on the extrapolated $^{10}Be/^{9}Be$ ratios below 5 mm depth.

3.2. Nd and Pb Isotope Time Series

[13] The three crusts display surface Pb and Nd isotope values ranging from 18.81 to 18.98 for $^{206}Pb/^{204}Pb$ and between −10.9 to −11.6 for ε_{Nd} (Table 3 and Figure 3). These values are in good agreement with values for other crust surfaces from the northeastern Atlantic [*Abouchami et al.*, 1999; *Reynolds et al.*, 1999; *Claude-Ivanaj et al.*, 2001]. Nevertheless, there are significant differences in the surface isotope ratios between the three crusts: Shallowest crust 3514-6, as well as crust 65GTV [*Abouchami et al.*, 1999] from 1500 m water depth at essentially the same location (Figures 1 and 4), show less radiogenic $^{206}Pb/^{204}Pb$ values (18.81 and 18.78, respectively) than the two deeper crusts (18.95 and 18.98). The time series of these four crusts are presented in Figure 4. All four crusts recorded essentially constant Pb isotope ratios prior to 4 Ma, whereas crusts 3514-6 and 3511-1 show values around 18.8 and 65GTV and 3513-14 recorded values around 18.7. After 4 Ma, the Pb isotope records of all crusts show a continuous increase in $^{206}Pb/^{204}Pb$ ratios similar to previously published records for other crusts from the eastern North Atlantic [*Abouchami et al.*, 1999; *Reynolds et al.*, 1999]. The only exception is shallowest crust 3514-6, which stayed constant. There is a significant trend in the amplitude of change over the past ~4 Ma with water depth from essentially constant $^{206}Pb/^{204}Pb$ values at 700–900 m depth to a maximum change of 0.25 in the deepest crust (3513-14), which started to change already at ~6 Ma (Table 4). There is no indication that the striking constancy of the Pb isotope time series of the shallowest crust does not reflect a seawater signal. Potential substrate dissolution can be excluded because the Pb isotope composition of volcanic rocks from the same and nearby seamounts is very different from that of seawater recorded by the crust [*Geldmacher et al.*, 2006]. In particular, the $^{207}Pb/^{204}Pb$ ratios (~15.50 to ~15.60) of the basaltic rocks are much lower than those of seawater derived from our samples, as well as from other hydrogenetic crusts in the area.

[14] The amplitudes and the timing of changes in the Nd isotope time series show significant differences among the crusts although, in contrast to the Pb isotopes, there is no clear trend in the amplitude of the changes with water depth. The shallowest crust shows a continuous overall decrease of 2 ε_{Nd}

Table 3. Pb and Nd Isotopic Compositions of the Crusts

Depth, mm	Mean Depth, mm	Age, Ma	$^{206}Pb/^{204}Pb$	$^{207}Pb/^{204}Pb$	$^{208}Pb/^{204}Pb$	$^{143}Nd/^{144}Nd$	1σ[a]	$\varepsilon_{Nd(T)}$
				3514-6				
0–0.5	0.25	0.18	18.811	15.679	38.880	0.512077	±3	−10.94
1–1.5	1.25	0.91	18.799	15.677	38.862	0.512091	±3	−10.67
2–2.5	2.25	1.64	18.791	15.679	38.860	0.512104	±3	−10.40
3–3.5	3.25	2.37	18.789	15.676	38.850	0.512113	±3	−10.22
4–4.5	4.25	3.10	18.798	15.677	38.857	0.512119	±2	−10.09
5–5.5	5.25	3.83	18.807	15.678	38.863	0.512119	±3	−10.08
6–6.5	6.25	4.56	18.804	15.674	38.853	0.512123	±3	−10.00
7–7.5	7.25	5.29	18.798	15.676	38.865	0.512117	±3	−10.11
7–7.5	7.25	5.29				0.512137	±5	−9.72
8–8.5	8.25	6.02	18.790	15.675	38.869	0.512125	±3	−9.94
9–9.5	9.25	6.75	18.786	15.674	38.867	0.512134	±2	−9.75
10–11	10.50	7.34	18.783	15.674	38.877	0.512134	±3	−9.76
12–13	12.50	8.15	18.781	15.674	38.883	0.512134	±2	−9.74
14–15	14.50	8.97	18.786	15.676	38.887	0.512146	±2	−9.51
16–17	16.50	9.79	18.795	15.679	38.890	0.512157	±3	−9.29
18–19	18.50	11.20	18.794	15.680	38.890	0.512159	±3	−9.24
20–21	20.50	12.80	18.788	15.680	38.878	0.512182	±4	−8.75
22–23	22.50	14.40	18.776	15.678	38.867	0.512160	±3	−9.17
23–24	23.25	15.00	18.778	15.681	38.874	0.512171	±3	−8.96
	23.00	15.20						
				3511-1				
0–0.5	0.25	0.20	18.956	15.686	39.040	0.512045	±3	−11.56
1–1.5	1.25	1.00	18.915	15.682	39.004	0.512036	±2	−11.73
2–2.5	2.25	1.80	18.873	15.680	38.953	0.512037	±3	−11.71
3–3.5	3.25	2.60	18.836	15.680	38.907	0.512044	±3	−11.55
4–4.5	4.25	3.40	18.811	15.678	38.868	0.512060	±2	−11.24
5–5.5	5.25	4.20	18.803	15.679	38.854			
5–5.5	5.25	4.20	18.803	15.679	38.864	0.512071	±2	−11.02
6–6.5	6.25	5.00	18.803	15.677	38.860	0.512078	±3	−10.87
7–7.5	7.25	5.80	18.805	15.676	38.860	0.512089	±3	−10.65
8–8.5	8.25	6.60	18.808	15.677	38.867	0.512093	±2	−10.57
9–9.5	9.25	7.40	18.801	15.674	38.865	0.512109	±3	−10.24
10–11	10.50	8.32	18.793	15.674	38.868	0.512102	±3	−10.37
11–12	11.50	8.81	18.795	15.675	38.874	0.512103	±2	−10.35
12–13	12.50	9.30	18.794	15.675	38.886	0.512107	±3	−10.26
13–14	13.50	9.79	18.785	15.672	38.881	0.512114	±3	−10.11
14–15	14.50	10.28	18.783	15.675	38.893	0.512120	±3	−9.99
15–16	15.50	10.77	18.790	15.674	38.885	0.512142	±3	−9.56
16–17	16.50	11.26	18.798	15.674	38.882	0.512152	±3	−9.36
17–18	17.50	11.75	18.804	15.676	38.886	0.512193	±3	−8.55
	18.00	12.00						
				3513-14				
0–0.5	0.25	0.14	18.982	15.689	39.090	0.512060	±3	−11.27
1–1.5	1.25	0.71	18.937	15.690	39.048	0.512047	±3	−11.53
2–2.5	2.25	1.28	18.886	15.685	38.970	0.512058	±3	−11.31
3–3.5	3.25	1.85	18.856	15.682	38.926	0.512066	±3	−11.16
4–4.5	4.25	2.41	18.845	15.681	38.916	0.512077	±3	−10.94
5–5.5	5.25	2.94	18.845	15.683	38.923	0.512068	±3	−11.11
6–6.5	6.25	3.16	18.836	15.678	38.903	0.512074	±3	−10.99
7–7.5	7.25	3.39	18.836	15.681	38.910	0.512068	±3	−11.11
8–8.5	8.25	3.61	18.834	15.680	38.902	0.512085	±3	−10.77
9–9.5	9.25	3.84	18.809	15.679	38.909	0.512088	±3	−10.71
10–11	10.50	4.12	18.807	15.678	38.898	0.512102	±3	−10.43
12–13	12.50	4.57	18.798	15.679	38.869	0.512119	±3	−10.09
14–15	14.50	5.02	18.771	15.672	38.836	0.512106	±3	−10.34
16–17	16.50	5.47	18.750	15.672	38.829	0.512126	±3	−9.95
18–19	18.50	5.92	18.732	15.670	38.814	0.512133	±3	−9.81
20–21	20.50	6.37	18.739	15.667	38.806	0.512154	±3	−9.40

Table 3. (continued)

Depth, mm	Mean Depth, mm	Age, Ma	$^{206}Pb/^{204}Pb$	$^{207}Pb/^{204}Pb$	$^{208}Pb/^{204}Pb$	$^{143}Nd/^{144}Nd$	1σ[a]	$\varepsilon_{Nd(T)}$
22–23	22.50	6.81	18.734	15.669	38.811	0.512168	±3	−9.12
24–25	24.50	7.26	18.730	15.672	38.809	0.512163	±3	−9.21
26–27	26.50	7.71	18.722	15.668	38.795	0.512163	±3	−9.20
28–29	28.50	8.16	18.727	15.671	38.808	0.512178	±4	−8.90
30–31	30.50	8.61	18.719	15.669	38.799	0.512160	±3	−9.27
32–33	32.50	9.06	18.720	15.670	38.805	0.512162	±3	−9.22
34–35	34.50	9.51	18.714	15.668	38.797	0.512163	±3	−9.20
36–37	36.50	9.96	18.699	15.668	38.791	0.512146	±2	−9.52
38–39	38.50	10.41	18.702	15.667	38.794	0.512158	±4	−9.29
40–41	40.50	10.86	18.707	15.669	38.803	0.512149	±2	−9.47
42–43	42.50	11.31	18.715	15.669	38.811	0.512162	±2	−9.22
	43.00	11.42						

[a] The σ values correspond to SEM.

units between 15 Ma and the present. The decrease from 4 Ma to the present amounted to ~0.8 ε_{Nd} units. The intermediate depth crust also shows a continuous trend between 12 Ma ago and the present, but the amplitude was higher (~3 ε_{Nd} units) and there was no significant decrease over the past 4 Ma. The deepest crust shows constant values between 11 and ~6 Ma followed by a decrease in ε_{Nd} from −9.5 to −11.5. This is the steepest gradient over the last ~4 Ma found in the

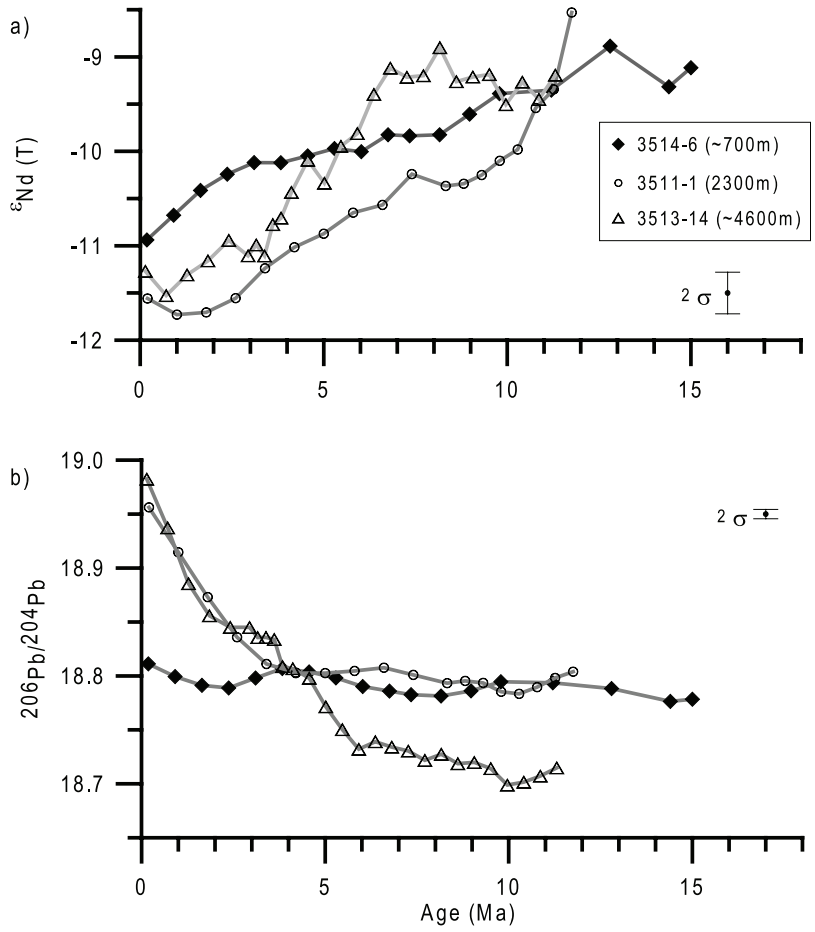

Figure 3. Time series of (a) $\varepsilon_{Nd(T)}$ and (b) $^{206}Pb/^{204}Pb$ versus age for the three crusts studied. All error bars represent $2\sigma_{(SD)}$ external reproducibilities of repeated standard measurements.

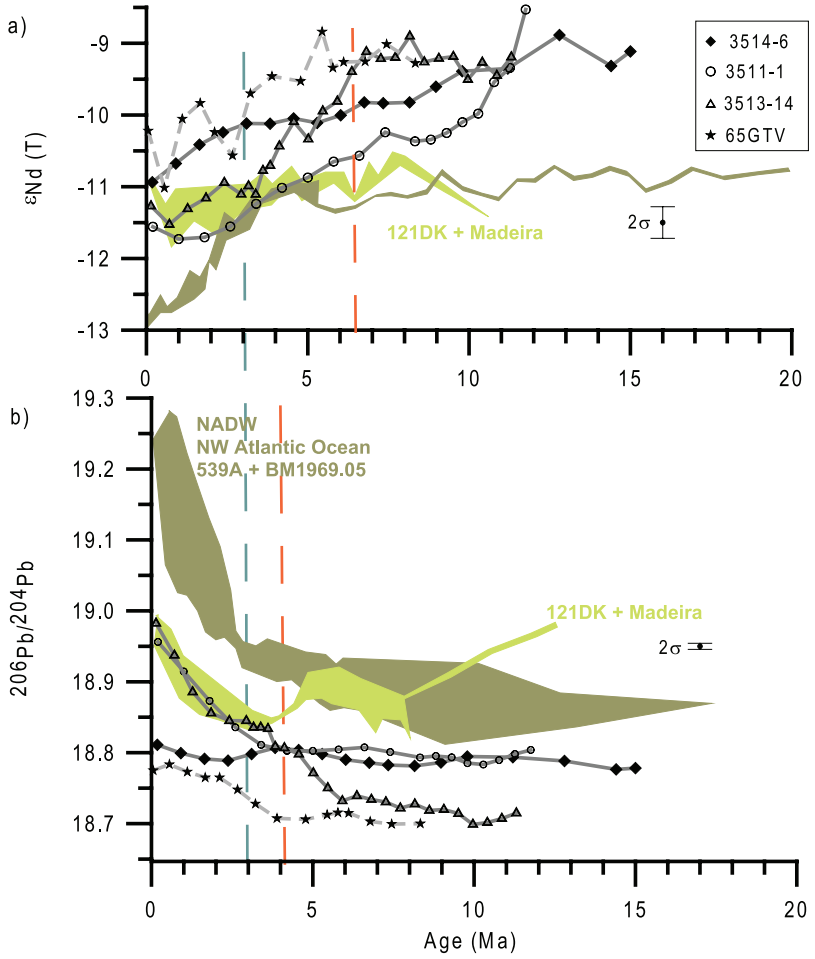

Figure 4. Comparison of (a) Nd and (b) $^{206}Pb/^{204}Pb$ time series for our three crusts with other crusts from the northeastern and northwestern Atlantic: The data for 65GTV [*Abouchami et al.*, 1999] are plotted as solid stars with dashed line. The data for 121DK [*Abouchami et al.*, 1999] and Madeira [*Reynolds et al.*, 1999] are plotted as a light green field. The data from the northwestern Atlantic crusts BM1969.05 (39°N; 61°W) and ALV 539 (35°N; 59°W) [*Burton et al.*, 1997, 1999; *Reynolds et al.*, 1999] are plotted as a dark green field. Dashed vertical lines mark the major changes in patterns for the northeastern Atlantic (red) and northwestern Atlantic (blue).

records of our crusts, which resembles the pattern in the western North Atlantic.

4. Discussion

4.1. Present-Day Situation

[15] The crust surface ε_{Nd} values are −10.9, −11.6 and −11.3 for crusts 3514-6, 3511-1, and 3513-14, respectively. Despite the fact that the surface data integrate over several 100 ka for each sample, the values are comparable to present-day water column data obtained at nearby locations [*Piegras and Wasserburg*, 1983; *Spivack and Wasserburg*, 1988; *Tachikawa et al.*, 2004]. Shallowest crust 3514-6 lies within the upper core of MOW and shows a Nd isotope signature (ε_{Nd} = −10.9) that agrees well with values for the corresponding water depth (ε_{Nd} = −10.6) of nearby water profile A-II 109, St. 95 [*Piegras and Wasserburg*, 1983] (Figures 1 and 5). In the water profile A-II 109, St. 95 the ε_{Nd} signature in the core of MOW, at 1000 m water depth, is −9.8, reflecting the presence of a large fraction of MOW at this location.

[16] The surfaces of the intermediate depth crust 3511-1 (corresponding to NEADW) and the deepest crust 3513-14 (NEADW, possibly recording minor AABW influence) show more negative ε_{Nd} values which are similar to the water column data reported for the corresponding water depths at A-II 109, St. 95 (−12.2 and −11.8, respectively) as well as for samples from a study further south in the eastern North Atlantic [*Tachikawa et al.*, 1999]. The data of the intermediate depth crust are also in good agreement with values published for other

Table 4. Overall Variations of Nd and Pb From ~4 Ma Toward the Present[a]

Sample	Water Depth, m	Location	ΔNd	Overall Change, ε_{Nd} Units	ΔPb
3514-6	688–938	Lion seamount	0.8	2.0	0.02
65GTV[b]	1500	Lion seamount	1.3	2.0	0.07
121DK[b]	2000	Tropic seamount	0.8	0.8	0.11
3511-1	2161–2436	Josephine seamount	0.6	3.0	0.15
3513-14	4586–4603	Madeira-Tore Rise	2.0	2.5	0.25
Madeira[c]	5347–4867	Madeira Abyssal Plain	0.3	0.0	0.15

[a] ΔNd and ΔPb correspond to the calculated variation of Nd and Pb values from the age that the sample start to vary toward the present. For all crusts the starting age of the major variation is ~4 Ma, whereas for deepest crust 3513-14 the start is at ~6 Ma. The overall change in ε_{Nd} values corresponds to the total variation through the profile.
[b] *Abouchami et al.* [1999].
[c] *Reynolds et al.* [1999].

crusts in the NE Atlantic: Crust 121DK (2000 m water depth) shows a ε_{Nd} surface value of −11.84, whereas the surface of crust 65GTV (1500 m water depth) shows a higher ε_{Nd} value of −10.2, in agreement with its proximity to the lower core of MOW [*Abouchami et al.*, 1999]. Data for the deepest crust agree with values for the surface of crust Madeira (~5100 m water depth) with an ε_{Nd} = −11.1 [*Reynolds et al.*, 1999].

[17] Preanthropogenic Pb isotopic data cannot be extracted from modern seawater. We therefore compare our $^{206}Pb/^{204}Pb$ surface values with surface data of other northeastern Atlantic crusts. Our shallowest crust (upper MOW core) shows a $^{206}Pb/^{204}Pb$ value of 18.81, comparable with the 18.78 value of crust 65GTV (lower MOW core), which are the least radiogenic crusts [*Abouchami et al.*, 1999]. The intermediate and deepest crusts show more radiogenic $^{206}Pb/^{204}Pb$ isotopic values of 18.96 and 18.98, respectively, which are comparable with values for crusts 121DK and Madeira (18.95 and 18.99, respectively) from similar water depths [*Abouchami et al.*, 1999; *Reynolds et al.*, 1999; *Claude-Ivanaj et al.*, 2001].

4.2. Mid-Miocene to Present Water Mass Evolution

[18] Previous studies have investigated Pb and Nd isotope time series in ferromanganese crusts from the western and eastern North Atlantic [*Burton et al.*, 1997, 1999; *O'Nions et al.*, 1998; *Abouchami et al.*, 1999; *Reynolds et al.*, 1999; *Claude-Ivanaj et al.*, 2001; *Frank et al.*, 2003]. Western North Atlantic records show a consistent evolution of Nd and Pb isotope time series for NADW or a precursor of it over the past 3 Ma, although apparent differences in the timing of change have been observed [*Burton et al.*, 1999]. Eastern North Atlantic data show similar patterns in Pb and Nd isotope records but different absolute values, as well as timing and amplitudes of change. The Pb isotope changes in the deep northeastern Atlantic occurred about 1 Ma earlier than in the western basin and are shifted by about 0.3 in $^{206}Pb/^{204}Pb$ toward less radiogenic ratios. There is a common decreasing trend in all the Nd isotope time series that resembles records from the western North Atlantic over the past 3 Ma [*Burton et al.*, 1997, 1999; *O'Nions et al.*, 1998]. However, our new deep-water Nd isotope record shows an early decrease in ε_{Nd} (~6 Ma) that is of similar amplitude as western North Atlantic records from 3 Ma

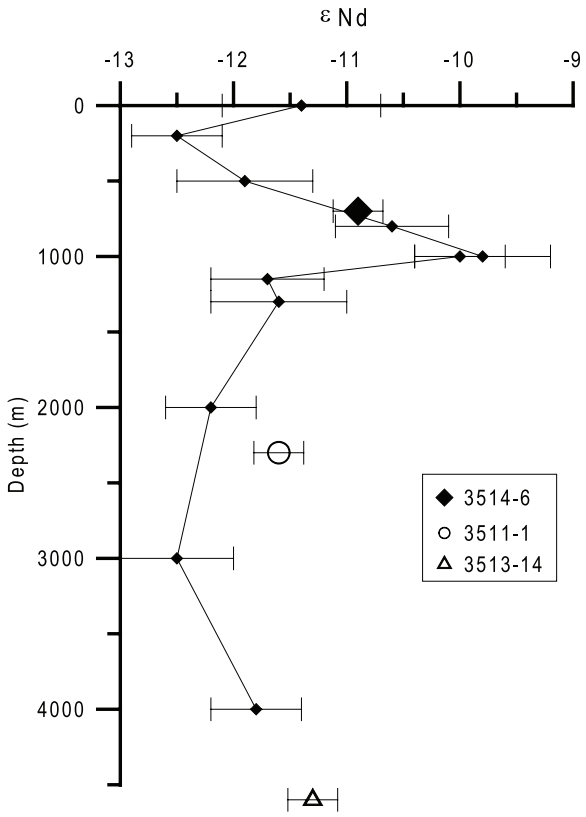

Figure 5. Plot of $\varepsilon_{Nd(0)}$ as a function of depth at station A-II, 109 St. 95 [*Piegras and Wasserburg*, 1983], compared with the ε_{Nd} of the surfaces of our three crusts (3514-6, 3511-1 and 3513-14).

to the present, but is ~1.5 ε_{Nd} units more radiogenic. The marked changes observed in the Pb and Nd compositions of western NADW and NEADW were interpreted as a consequence of changes of style and intensity of continental weathering in northern Canada and Greenland or alternatively as a change in the signatures and contributions of water masses mixing to produce NADW since the onset of NHG 2.7 Ma ago [*Burton et al.*, 1997, 1999; *O'Nions et al.*, 1998; *Reynolds et al.*, 1999; *Foster and Vance*, 2006]. Increased mechanical weathering was invoked as the cause of increased erosional input of old cratonic material with low ε_{Nd}, which may have led to the decrease of ε_{Nd} in North Atlantic deep waters over the past 3 Ma [*O'Nions et al.*, 1998]. Alternatively, the contribution of LSW with its very unradiogenic Nd isotope composition may have increased over the past 3 Ma [*Burton et al.*, 1999]. Enhanced release of loosely bound radiogenic Pb from old cratonic rocks (incongruent weathering), rapidly eroded under glacial conditions, has been inferred to be the cause for the drastic increase in $^{206,207,208}Pb/^{204}Pb$ over the past 3–2 Ma [*von Blanckenburg and Nägler*, 2001; *Foster and Vance*, 2006]. Despite the fact that the time series patterns of the eastern North Atlantic crusts generally resemble those of the western basin, it appears that the eastern North Atlantic led the major changes in Nd and Pb isotope compositions in three crusts from water depths between 1500 and 4600 m by about 1–3 Ma, which cannot be the result of dating uncertainties. This difference in timing cannot be explained by changes in weathering in northern Canada and Greenland associated with the onset of NHG but must rather have been associated with paleoceanographic changes that occurred prior to and during the early phase of the onset of NHG. These changes may for example have been related to the closure of the Isthmus of Panama. It has been reported that the gradual closure of the Isthmus of Panama had a major impact on intermediate and deep water circulation and an intensification of NADW export at ~4.6 Ma [*Driscoll and Haug*, 1998; *Frank et al.*, 1999b; *Reynolds et al.*, 1999]. The early change in the eastern North Atlantic may thus have been caused by a diminished influence of LDW as suggested by *Abouchami et al.* [1999]. There is, however, no clearly detectable shift toward less radiogenic Nd isotope and more radiogenic Pb isotope composition at 4 Ma in the records from the Romanche and Vema fracture zones, the ultimate pathway of southern sourced water masses in the eastern North Atlantic Basin [*Frank et al.*, 2003]. More likely, therefore, the similarity of the overall patterns and the differences in amplitudes observed for Pb and Nd isotopes between the western and eastern basins over the past 4 Ma indicate an influence from efficient deep water mass exchange between the two basins via a northern route, such as the Charlie-Gibbs Fracture Zone (CGFZ) [*Sy et al.*, 1997; *Paillet et al.*, 1998; *Bower et al.*, 2002]. In the more distant past (prior to ~2 Ma), the CGFZ could have dominated the exchange between the two basins. This may have enabled a pronounced early and direct transfer of the extremely unradiogenic Nd and radiogenic Pb isotope signature of LSW into the northeastern Atlantic basin prior to the change in the isotopic composition of NADW. This is supported by model calculations [*Sy et al.*, 1997] which show that spreading of LSW under winter forcing conditions can occur at a more southerly location, leading to a more efficient export of this water mass to the eastern basin via northern fracture zones such as the CGFZ. *Schott et al.* [1999] reported the existence of phases of strong deep eastward flow through the CGFZ under present-day conditions. These authors conclude that the North Atlantic Current (NAC, which is a warm surface current transporting Gulf Stream waters to the eastern North Atlantic), also plays a crucial role for the pathways of deep water supply out of the eastern North Atlantic. According to their observations, if the NAC follows a more northerly route for an extended period of time, then the flow through the CGFZ can be pushed backward, thus changing the composition of the northern deep circulation system. Moreover, *Boessenkool et al.* [2007] pointed out that convective change in the Labrador Sea may be more important in the production of NADW than Greenland-Scotland Ridge (GSR) overflows, as the volume transport of the GSR overflows weakens when LSW formation intensifies. A scenario like this may explain the earlier and pronounced LSW influence we observe in the eastern basin records. It is interesting to note in this context that *Wright and Miller* [1996] suggested a correlation between the uplift of the GSR and reduced export of Northern Component Water (which is the precursor of NADW) also pointing toward a potentially more LSW dominated Northern Component Water in the past. *Thomas and Via* [2007] recently suggested that a rapid decrease in the Nd isotope signal in the Walvis Ridge of the southeastern Atlantic between 10.6 and 7.3 Ma, may have been caused by deep convection in the Labrador Sea and a corresponding change in the Nd isotope composition of NADW. Such a very

early change is not observed in other equatorial and Southern Atlantic records but our shallow and intermediate records clearly also show a decrease in the Nd isotope signal since ~12 Ma (Figure 3a) that may already have been related to increased contributions from the Labrador Sea.

[19] There is a clear similarity in the Pb and Nd pattern between the two shallowest records from the northeastern Atlantic, crusts 3514-6 and 65GTV, in that they show less radiogenic $^{206}Pb/^{204}Pb$ ratios and more radiogenic ε_{Nd} values than the other crusts from the northeastern Atlantic over the past 3 Ma (Figure 4). The continuous increase in $^{206}Pb/^{204}Pb$ from 4 Ma to present has the largest amplitude in the deeper crusts, which appears to have been controlled by an increasing direct influence of LSW on the Pb isotope signature at depth. The change in Pb isotopes in the deepest crust even appears to have started as early as 6 Ma. In contrast, the Nd isotopes show no systematic change with water depth. This may be due to the shorter residence time of Pb compared with Nd, which is more efficiently mixed in the ocean. More importantly, the original Pb isotope end-member signature of LSW has probably been even more extreme than that of the Nd isotopes, which is why such a strong and clearly resolvable LSW signal is observed at depth. Small differences in Pb isotope composition between the crusts prior to 4 Ma probably originated from local input sources. In general, however, the deep water Pb isotope signature in the eastern North Atlantic Basin seems to have been dominated by water mass mixing, consistent with the general assumption that the adsorption of Pb onto particles is not reversible [*Henderson and Maier-Reimer*, 2002, and references therein], which means that there has been no significant release of surface water Pb or dust-derived Pb to deep waters.

4.3. Influence of MOW and the Messinian Salinity Crisis

[20] The Pb isotope time series of the shallowest crust 3514-6 is markedly different from all other time series in the North Atlantic and thus requires additional discussion. The relatively unradiogenic Pb isotope composition of this crust and crust 65GTV from 1500 m water depth is in agreement with the expected signal of MOW based on the geology of the continental landmasses surrounding the Mediterranean [*Abouchami et al.*, 1999]. The shallowest crust is located within the upper core of the MOW around 800 m depth [*Ambar et al.*, 1999, 2002] and the long-term stability of the signal indicates a continuous presence of MOW at this location and water depth, integrated over glacial/interglacial timescales, over the past 15 Ma. There is no indication of any significant growth hiatus during the MSC (Figure 2), which would, however, also be difficult to detect in view of the coarse resolution of the $^{10}Be/^{9}Be$ data. This apparently contrasts the missing record of the MSC between 6 and 5.3 Ma [*Krijgsman et al.*, 1999], when the Atlantic-Mediterranean exchange was reduced in comparison to the present-day [*Flecker and Ellam*, 2006]. The continuous and invariable Pb isotope record may indicate that the Pb isotopes were controlled by advection of MOW combined with local external inputs, such as partial dissolution of detrital particles from the nearby continents (e.g., Saharan dust) [*Abouchami et al.*, 1999; *Tachikawa et al.*, 1999]. In addition, there may be no indication of the MSC because MOW formed at least episodically and the corresponding isotopic signal reached the depth and location of crust 3514-6 during these short episodes. In fact, *Flecker et al.* [2002] and *Flecker and Ellam* [2006] argued that even during the deposition of the Upper Evaporite sequence in the Mediterranean, the outflow into the Atlantic was reduced but was not completely or continuously stopped. In support of this, *Flecker et al.* [2002] suggested that a complete isolation over the MSC is inconsistent with observed Sr isotopic offsets from coeval open marine values and the high salinities required for evaporite precipitation. In order to explain the evaporite deposition during the MSC, *Flecker and Ellam* [2006] proposed an alternative hypothesis to the desiccation or connected basin hypothesis which states that evaporite deposition was triggered by one, or potentially several, Atlantic transgressions that increased the mass of salt in the Mediterranean. In view of these results, it appears most likely that MOW formed episodically and that therefore the Pb and Nd isotope signatures, which integrate over several 100 ka, did not record short-term changes caused by the MSC. It is stressed here that the Pb isotopes recorded the continuous MOW signature (combined with some external contributions most likely from dust) due to the short residence time of Pb at this location proximal to the Strait of Gibraltar, whereas the Nd isotope record was overprinted by mixing with other North Atlantic water masses due its longer residence time.

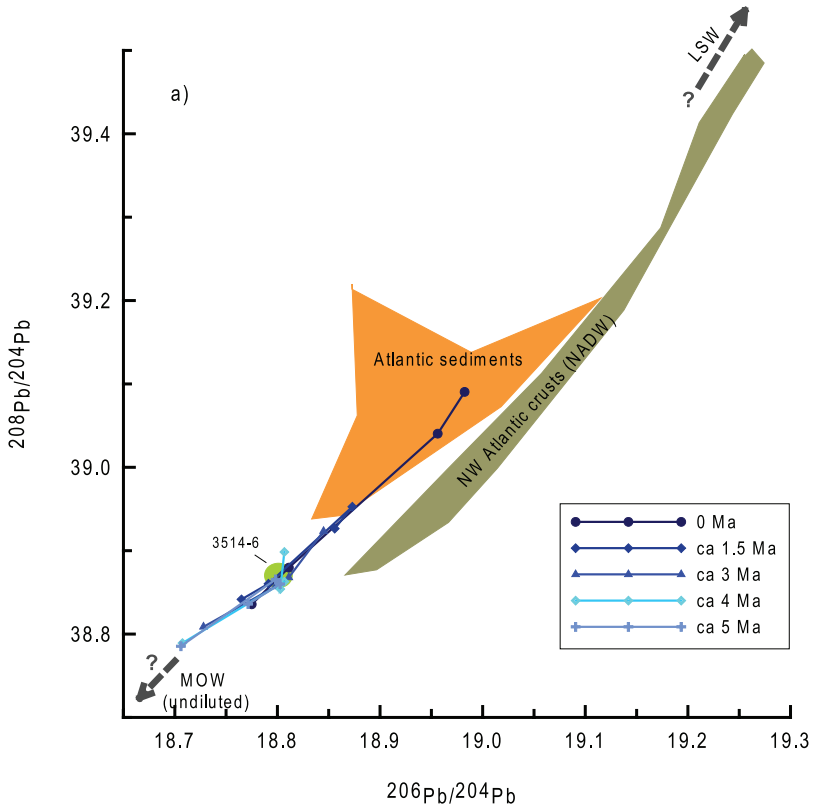

Figure 6. Time slice connections (surface, 1.5, 3, 4, and 5 Ma) from the northeastern Atlantic crusts (65GTV, 3514-6, 3511-1, and 3513-14) in (a) $^{208}Pb/^{204}Pb$ versus $^{206}Pb/^{204}Pb$ and (b) $^{207}Pb/^{204}Pb$ versus $^{206}Pb/^{204}Pb$ space. The lines mark connections between the data of particular time slices (the legend in the graphics displays each time slice color). The green ellipse displays the field of crust 3514-6; it shows a nearly constant Pb isotope signature. The symbols and fields for the potential sources influencing the study area are (1) NW Atlantic crusts data (dark green field) defined by data from BM1969.05 and ALV539 [*Burton et al.*, 1997, 1999; *Reynolds et al.*, 1999] for the time range 0–5 Ma; (2) data from Atlantic sediments, interpreted as Saharan dust (orange field) is given by *Sun* [1980]; and (3) Saharan dust data (open grey diamond) is given by B. Hamelin (personal communication, 2003). The dashed dark grey lines indicate the possible end-member compositions of unmodified MOW (unradiogenic) and LSW (radiogenic) end-members.

4.4. Pliocene-Pleistocene Evolution of Water Masses From Pb Isotopes

[21] In order to identify the changes in the sources of Pb contributing to seawater Pb isotope compositions over the past 5 Ma, time slice reconstructions of the four crusts in the eastern North Atlantic, which essentially only differ in water depth, were carried out (Figure 6). The time slice plots show that the Pb isotope ratios of all crusts can essentially be explained by a mixture between two water masses, the proportions of which changed over time (circa 5 Ma, circa 4 Ma, circa 3 Ma, circa 1.5 Ma, and present). The unradiogenic end-member has been MOW for the two shallow locations, whereas the radiogenic end-member most likely has been NEADW (including LDW and a LSW component). In addition, an external source, most likely dust, must have contributed to the Pb isotope signatures. For the present-day situation, the Pb in crust 65GTV is the least radiogenic. It is emphasized here that the MOW field represents an already modified isotope composition which is based only on the data for crust 65GTV from 1500 m water depth [*Abouchami et al.*, 1999]. It is most likely that unmodified MOW is even less radiogenic (Figure 6).

[22] Data for the interval 5 to 3 Ma indicate a dominance of the unradiogenic end-member, which then shift toward the radiogenic end-member, most pronouncedly for the present-day. At around 1.5 Ma, a composition intermediate between the two end-members was reached, but was accompanied by a change in slope (see particularly Figure 6b). Despite the overall similarity of the data, this indicates a change in the contributing end-members. Aridity increased in the Saharan

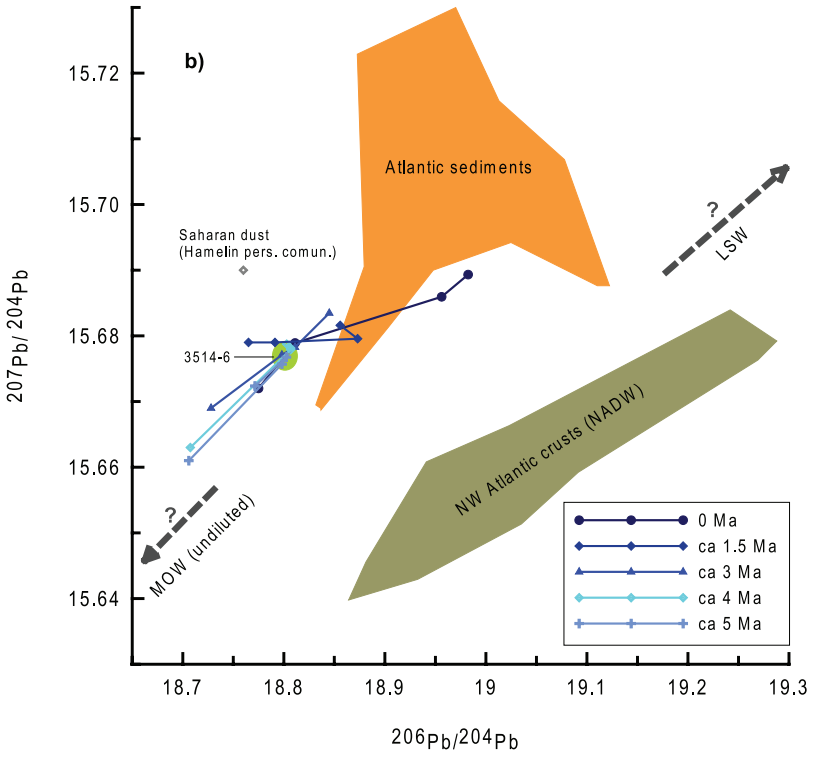

Figure 6. (continued)

region since ~4 Ma [*Rea*, 1994] caused by repeated cooling during the Pliocene-Pleistocene. A change in the source area of the Sahara from which dust was derived may have changed the mixing proportions of Pb at 1.5 Ma. Partial dissolution of dust may also have contributed to the markedly constant Pb isotope composition of the shallowest crust. In support of this, the data for the shallowest crust plot on the 1.5 Ma time slice line for the entire period between 5 Ma and the present. As the Pb residence time in the surface waters is very short, and because adsorption of Pb onto particles is in general not reversible [*Henderson and Maier-Reimer*, 2002], the Pb isotope signature of the upper part of MOW, as recorded by the shallowest crust, must have been strongly influenced by dust inputs. In contrast the deep water Pb isotope composition was mainly controlled by ocean circulation and water mass mixing.

4.5. Alternative Age Model and Implications for the Shallow Crust Record

[23] As mentioned in section 3.1., there is a possibility arising from its low surface $^{10}Be/^{9}Be$ ratio that the uppermost 2 mm of shallowest crust 3514-6, corresponding to ~1.5 Ma of growth, are missing due to erosion or dissolution. This would mean that this crust does have a relatively radiogenic ε_{Nd} value at the surface, previously interpreted as MOW influence. It would also imply that the decrease of the Nd isotopes at shallow depths started even 1.5 Ma earlier. In the case of Pb isotopes the record would still be very similar to the intermediate crust record prior to 4 Ma and remain constant until 1.5 Ma. Although such an erosional event cannot be completely excluded, the macroscopic evidence and the expected lower $^{10}Be/^{9}Be$ ratio at this water depth clearly argue against it. In addition, the Nd isotope signature of the surface of the crust agrees very well with values for the corresponding water depth of the water profile A-II 109, St. 95 [*Piegras and Wasserburg*, 1983] (Figure 5), which is why we consider the surface of this crust to be the true growth surface. However, even if there was an erosion or dissolution event, the overall interpretations of the Pb and Nd isotope ratios presented in sections 4.1.–4.4. would not significantly change.

5. Conclusions

[24] We present new time series of the Pb and Nd isotope evolution of water masses at different depths from the eastern North Atlantic of the past 15 Ma. The similarity between the Pb and Nd time series patterns from the northeastern and north-

western Atlantic over the past 4 Ma shows that there has been efficient mixing between the two basins. This and the fact that the northeastern Atlantic shows a major change in the trends 1–3 Ma earlier, reinforces the idea of an efficient export of LSW to the eastern Atlantic via a northern route such as across the CGFZ rather than through the equatorial fractures zones [*Abouchami et al.*, 1999; *Frank et al.*, 2003]. A continuous decreasing trend in the Nd isotope composition at shallow and intermediate depths may indicate that waters from the Labrador Sea started to influence the eastern North Atlantic basin as early as at 12 Ma.

[25] The evolution of water mass mixing, from ~5 Ma to the present, as reconstructed from Pb isotopes, can be explained by a mixture between two principal end-members: an unradiogenic MOW end-member and a radiogenic NEADW end-member. It is likely that a local external input has influenced the Pb isotope evolution of the MOW. This is indicated by the invariant Pb isotope composition of the shallowest crust, located within the modern MOW, which is intermediate between the inferred undiluted MOW and NEADW end-members. This is probably due to the release of Pb from Saharan dust resulting from higher dust fluxes as a consequence of enhanced aridity. This crust has recorded an essentially constant MOW signal, despite the fact that the MSC occurred. This indicates that MOW was at least released episodically during that time and that the cessations of MOW were too short to be resolved in the ferromanganese crust record.

[26] The enhanced $^{206}Pb/^{204}Pb$ gradient with water depth over the past ~4 Ma (Table 4) that we observe in our time series can best be explained by a stronger influence of LSW-derived Pb in the deeper crusts indicating that the Pb isotope composition of LSW must have been extremely radiogenic. Thus the Pb isotope compositions of the shallower water masses have been controlled by a combination of local water mass mixing and external sources, such as dust, whereas those of the deeper water masses were mainly controlled by ocean circulation and water mass mixing.

Acknowledgments

[27] We thank the Portuguese Science and Technology Foundation (FCT) for financial support of the projects INGMAR and PDCT/MAR/56823/2004. S.B.M. was supported by grant INGMAR-BICGEOQ1 and now grant SFRH/BD/22263/2005, both from FCT. We would also like to thank GRICES (Portugal) and DAAD (Germany) for traveling support. The $^{10}Be/^{9}Be$ ratios were measured at the Zurich AMS Facility jointly operated by the Swiss Federal Institute of Technology, Zurich and Paul Scherrer Institute, Villigen, Switzerland. The crew and scientific party of Meteor M51/1 cruise are also thanked as well as the Deutsche Forschungsgemeinschaft (DFG, German Research Council) for funding and Socfac program (National Oceanography Center, Southampton, U.K.) for ICP-MS/AES analyses. We also thank J. Fischer and L. Stramma for discussions and Mário Mil-Homens for help with the graphics. The editor Vincent Salters, as well as Ben Reynolds and one anonymous reviewer are thanked for their contribution to the improvement of the quality of this paper.

References

Abouchami, W., and S. L. Goldstein (1995), A lead isotopic study of Circum-Antarctic manganese nodules, *Geochim. Cosmochim. Acta*, *59*(9), 1809–1820.

Abouchami, W., S. J. G. Galer, and A. Koschinsky (1999), Pb and Nd isotopes in NE Atlantic Fe-Mn crusts: Proxies for metal paleosources and paleocean circulation, *Geochim. Cosmochim. Acta*, *63*(10), 1489–1505.

Ambar, I., and M. R. Howe (1979), Observations of the Mediterranean outflow-I Mixing in the Mediterranean Outflow, *Deep Sea Res., Part I*, *26A*, 535–554.

Ambar, I., L. Armi, A. Bower, and T. Ferreira (1999), Some aspects of time variability of the Mediterranean Water off south Portugal, *Deep Sea Res., Part I*, *46*, 1109–1136.

Ambar, I., N. Serra, M. J. Brogueira, G. Cabeçadas, F. Abrantes, P. Freitas, C. Gonçalves, and N. Gonzalez (2002), Physical, chemical and sedimentological aspects of the Mediterranean outflow off Iberia, *Deep Sea Res., Part II*, *49*, 4163–4177.

Bartoli, G., M. Sarnthein, M. Weinelt, H. Erlenkeuser, D. Garbe-Schonberg, and D. W. Lea (2005), Final closure of Panama and the onset of Northern Hemisphere glaciation, *Earth Planet. Sci. Lett.*, *237*, 33–44.

Belshaw, N. S., P. A. Freedman, R. K. O'Nions, M. Frank, and Y. Guo (1998), A new variable dispersion double-focusing plasma mass spectrometer with performance illustrated for Pb isotopes, *Int. J. Mass Spectrom.*, *181*(1–3), 51–58.

Bertram, C. J., and H. Elderfield (1993), The geochemical balance of the rare earth elements and neodymium isotopes in the oceans, *Geochim. Cosmochim. Acta*, *57*, 1957–1986.

Boessenkool, K. P., I. R. Hall, H. Elderfield, and I. Yashayaev (2007), North Atlantic climate and deep-ocean flow speed changes during the last 230 years, *Geophys. Res. Lett.*, *34*, L13614, doi:10.1029/2007GL030285.

Bower, A. S., B. L. Cann, T. Rossby, W. Zenk, J. Gould, K. Speer, P. L. Richardson, M. D. Prater, and H.-M. Zhang (2002), Directly measured mid-depth circulation in the northeastern North Atlantic Ocean, *Nature*, *419*, 603–607.

Broecker, W. S., C. Rooth, and T.-H. Peng (1985), Ventilation of the deep northeastern Atlantic, *J. Geophys. Res.*, *90*, 6940–6944.

Brown, E. T., C. I. Measures, J. M. Edmond, D. L. Bourlès, G. M. Raisbeck, and F. Yiou (1992), Continental inputs of beryllium to the oceans, *Earth Planet. Sci. Lett.*, *114*, 101–111.

Burton, K. W., H.-F. Ling, and R. K. O'Nions (1997), Closure of the Central American Isthmus and its effect on deep-water formation in the North Atlantic, *Nature*, *386*, 382–385.

Burton, K. W., D.-C. Lee, J. N. Christensen, A. N. Halliday, and J. R. Hein (1999), Actual timing of neodymium isotopic variations recorded by Fe-Mn crusts in the western North Atlantic, *Earth Planet. Sci. Lett.*, *171*, 149–156.

Claude-Ivanaj, C., A. W. Hofmann, I. Vlastélic, and A. Koschinsky (2001), Recording changes in ENADW composition over the last 340 ka using high precision lead isotopes in a Fe-Mn crust, *Earth Planet. Sci. Lett.*, *188*, 73–89.

Cohen, A. S., R. K. O'Nions, R. Siegenthaler, and W. L. Griffin (1988), Chronology of the pressure-temperature history recorded by a granulite terrain, *Contrib. Mineral. Petrol.*, *98*, 303–311.

Davies, R., J. Cartwright, J. Pike, and C. Line (2001), Early Oligocene initiation of North Atlantic Deep Water formation, *Nature*, *410*, 917–920.

Driscoll, N. W., and G. H. Haug (1998), A short circuit in thermohaline circulation: A cause for Northern Hemisphere glaciation, *Science*, *282*(5388), 436–438.

Flecker, R., and R. M. Ellam (2006), Identifying late Miocene episodes of connection and isolation in the Mediterranean-Paratethyan realm using Sr isotopes, *Sediment. Geol.*, *188–189*, 189–203.

Flecker, R., S. D. Villiers, and R. M. Ellam (2002), Modelling the effect of evaporation on the salinity-$^{87}Sr/^{86}Sr$ relationship in modern and ancient marginal-marine systems: The Mediterranean Messinian Salinity Crisis, *Earth Planet. Sci. Lett.*, *203*, 221–233.

Foster, G. L., and D. Vance (2006), Negligible glacial-interglacial variation in continental chemical weathering rates, *Nature*, *444*, 918–921.

Frank, M. (2002), Radiogenic isotopes: Tracers of past ocean circulation and erosional input, *Rev. Geophys.*, *40*(1), 1001, doi:10.1029/2000RG000094.

Frank, M., R. K. O'Nions, J. R. Hein, and V. K. Banakar (1999a), 60 Myr records of major elements and Pb-Nd isotopes from hydrogenous ferromanganese crusts: Reconstruction of seawater paleochemistry, *Geochim. Cosmochim. Acta*, *63*, 1689–1708.

Frank, M., B. C. Reynolds, and R. K. O'Nions (1999b), Nd and Pb isotopes in Atlantic and Pacific water masses before and after the closure of the Panama gateway, *Geology*, *27*, 1147–1150.

Frank, M., N. Whiteley, S. Kasten, J. R. Hein, and K. O'Nions (2002), North Atlantic Deep Water export to the Southern Ocean over the past 14 Myr: Evidence from Nd and Pb isotopes in ferromanganese crusts, *Paleoceanography*, *17*(2),1022, doi:10.1029/2000PA000606.

Frank, M., T. van de Flierdt, A. N. Halliday, P. W. Kubik, B. Hattendorf, and D. Günther (2003), Evolution of deep-water mixing and weathering inputs in the central Atlantic Ocean over the past 33 Myr, *Paleoceanography*, *18*(4), 1091, doi:10.1029/2003PA000919.

Galer, S. J. G., and R. K. O'Nions (1989), Chemical and isotopic studies of ultramafic inclusions from the San Carlos volcanic field, Arizona: A bearing on their petrogenesis, *J. Petrol.*, *30*, 1033–1064.

Geldmacher, J., K. Hoernle, A. Klügel, P. van den Bogaard, F. Wombacher, and B. Berning (2006), Origin and geochemical evolution of the Madeira-Tore Rise (eastern North Atlantic), *J. Geophys. Res.*, *111*, B09206, doi:10.1029/2005JB003931.

Grousset, F. E., P. E. Biscaye, A. Zindler, J. Prospero, and R. Chester (1988), Neodymium isotopes as tracers in marine sediments and aerosols: North Atlantic, *Earth Planet. Sci. Lett.*, *87*, 367–378.

Hein, J. R., A. Koschinsky, M. Bau, F. T. Manheim, J.-K. Kang, and L. Roberts (2000), Cobalt-rich ferromanganese crusts in the Pacific, in *Handbook of Marine Mineral Deposits*, edited by D. S. Cronan, pp. 239–279, CRC Press, Boca Raton, Fla.

Henderson, G., and E. Maier-Reimer (2002), Advection and removal of ^{210}Pb and stable Pb isotopes in the oceans: A general circulation model study, *Geochim. Cosmochim. Acta*, *66*, 257–272.

Hoernle, K., and Scientific Party (2003), Cruise Report M51/1, in *Ostatlantik-Mittelmeer-Schwarzes Meer, Cruise No. 51, 12 September–28 December 2001*, *Meteor-Ber. 03-1*, edited by C. Hemleben et al., pp. 3–35, Univ. Hamburg, Hamburg, Germany.

Hofmann, H. J., J. Beer, G. Bonani, H. R. von Gunten, S. Raman, M. Suter, R. L. Walker, W. Wölfli, and D. Zimmermann (1987), ^{10}Be: Half-life and AMS-standards, *Nucl. Instrum. Methods Phys. Res., Sect. B*, *29*, 32–36.

Jeandel, C. (1993), Concentration and isotopic composition of Nd in the southern Atlantic Ocean, *Earth Planet. Sci. Lett.*, *117*, 581–591.

Johannesson, K. H., and D. J. Burdige (2007), Balancing the global oceanic neodymium budget: Evaluating the role of groundwater, *Earth Planet. Sci. Lett.*, *253*, 129–142.

Johnson, R. G. (1997), Ice age initiation by an ocean-atmospheric circulation change in the Labrador Sea, *Earth Planet. Sci. Lett.*, *148*, 367–379.

Klemm, V., S. Levasseur, M. Frank, J. R. Hein, and A. N. Halliday (2005), Osmium isotope stratigraphy of a marine ferromanganese crust, *Earth Planet. Sci. Lett.*, *238*, 42–48.

Koschinsky, A., P. Halbach, J. R. Hein, and A. Mangini (1996), Ferromanganese crusts as indicators for paleoceanographic events in the NE Atlantic, *Geol. Rundsch.*, *85*, 567–576.

Krijgsman, W., F. J. Hilgen, I. Raffi, F. J. Sierro, and D. S. Wilson (1999), Chronology, causes and progression of the Messinian salinity crisis, *Nature*, *400*, 652–655.

Ku, T. L., M. Kusakabe, C. I. Measures, J. R. Southon, G. Cusimano, J. S. Vogel, D. E. Nelson, and S. Naraya (1990), Beryllium isotope distribution in the western North Atlantic: A comparison to the Pacific, *Deep Sea Res.*, *37*(5), 795–808.

Lacan, F., and C. Jeandel (2005a), Acquisition of the neodymium isotopic composition of the North Atlantic Deep Water, *Geochem. Geophys. Geosyst.*, *6*, Q12008, doi:10.1029/2005GC000956.

Lacan, F., and C. Jeandel (2005b), Neodymium isotopes as a new tool for quantifying exchange fluxes at the continent-ocean interface, *Earth Planet. Sci. Lett.*, *232*, 245–257.

Madelain, F. (1970), Influence de la topographie du fond sur l'écoulement Mediterranéen entre le Détroit de Gibraltar et le cap saint-Vincent, *Cah. Oceanogr.*, *22*, 43–61.

Maden, C., M. Doebeli, P. W. Kubik, M. Frank, and M. Suter (2004), Measurement of carrier-free ^{10}Be samples in AMS: The method and its potential, *Nucl. Instrum. Methods Phys. Res., Sect. B*, *223–224*, 247–252.

Manheim, F. T. (1986), Marine cobalt resources, *Science*, *232*, 600–608.

Martin, E. E., and H. D. Scher (2004), Preservation of seawater Sr and Nd isotopes in fossil fish teeth: Bad news and good news, *Earth Planet. Sci. Lett.*, *220*, 25–39.

Murdock, T. Q., A. J. Weaver, and A. F. Fanning (1997), Paleoclimatic response of the closing of the Isthmus of Panama in a coupled ocean-atmosphere model, *Geophys. Res. Lett.*, *24*, 253–256.

O'Nions, R. K., M. Frank, F. von Blanckenburg, and H.-F. Ling (1998), Secular variation of Nd and Pb isotopes in ferromanganese crusts from the Atlantic, Indian and Pacific oceans, *Earth Planet. Sci. Lett.*, *155*, 15–28.

Paillet, J., M. Arhan, and M. S. McCartney (1998), Spreading of Labrador Sea Water in the eastern North Atlantic, *J. Geophys. Res.*, *103*, 10,223–10,239.

Piegras, D. J., and S. B. Jacobsen (1988), The isotopic composition of neodymium in the North Pacific, *Geochim. Cosmochim. Acta*, *52*, 1373–1381.

Piegras, D. J., and G. J. Wasserburg (1982), Isotopic composition of neodymium in waters from the Drake Passage, *Science*, *217*, 207–214.

Piegras, D. J., and G. J. Wasserburg (1983), Influence of the Mediterranean Outflow on the isotopic composition of neodymium in waters of the North Atlantic, *J. Geophys. Res.*, *88*, 5997–6006.

Piegras, D. J., and G. J. Wasserburg (1987), Rare earth transport in the western North Atlantic inferred from isotopic observations, *Geochim. Cosmochim. Acta*, *51*, 1257–1271.

Ravelo, A. C., and D. H. Andreasen (2000), Enhanced circulation during a warm period, *Geophys. Res. Lett.*, *27*, 1001–1004.

Raymo, M. E., D. Hodell, and E. Jansen (1992), Response of deep ocean circulation to initiation of northern hemisphere glaciation (3–2 Ma), *Paleoceanography*, *7*, 645–672.

Rea, D. K. (1994), The paleoclimatic record provided by eolian deposition in the deep sea: The geologic history of wind, *Rev. Geophys.*, *32*, 159–195.

Reid, J. L. (1978), On the mid-depth circulation of the salinity field in the North Atlantic Ocean, *J. Geophys. Res.*, *83*, 5063–5067.

Reynolds, B. C., M. Frank, and R. K. O'Nions (1999), Nd- and Pb-isotope time series from Atlantic ferromanganese crusts: Implications for changes in provenance and paleocirculation over the last 8 Myr, *Earth Planet. Sci. Lett.*, *173*, 381–396.

Rogerson, M., E. J. Rohling, and P. P. E. Weaver (2006), Promotion of meridional overturning by Mediterranean-derived salt during the last deglaciation, *Paleoceanography*, *21*, PA4101, doi:10.1029/2006PA001306.

Scher, H. D., and E. E. Martin (2006), Timing and climatic consequences of the opening of Drake Passage, *Science*, *312*, 428–430.

Schmitz, W. J., and M. S. McCartney (1993), On the North Atlantic circulation, *Rev. Geophys.*, *31*, 29–49.

Schott, F., L. Stramma, and J. Fischer (1999), Interaction of the North Atlantic Current with the deep Charlie Gibbs Fracture Zone throughflow, *Geophys. Res. Lett.*, *26*, 369–372.

Spivack, A. J., and G. J. Wasserburg (1988), Neodymium isotopic composition of the Mediterranean outflow and the eastern North Atlantic, *Geochim. Cosmochim. Acta*, *52*, 2767–2773.

Stordal, M. C., and G. J. Wasserburg (1986), Neodymium isotopic study of Baffin Bay water: Sources of REE from very old terranes, *Earth Planet. Sci. Lett.*, *77*, 259–272.

Sun, S.-S. (1980), Lead isotopic study of young volcanic rocks from mid-ocean ridges, ocean islands and island arcs, *Philos. Trans. R. Soc. London, Ser. A*, *297*, 409–445.

Sy, A., M. Rhein, J. R. N. Lazier, K. P. Koltermann, J. Meincke, and A. Putzka (1997), Surprisingly rapid spreading of newly formed intermediate waters across the North Atlantic Ocean, *Nature*, *386*, 675–679.

Tachikawa, K., C. Jeandel, and B. Dupré (1997), Distribution of rare earth elements and neodymium isotopes in settling particulate material of the tropical Atlantic Ocean (EUMELI site), *Deep Sea Res., Part I*, *44*, 1769–1792.

Tachikawa, K., C. Jeandel, and M. Roy-Barman (1999), A new approach to the Nd residence time in the ocean: The role of atmospheric inputs, *Earth Planet. Sci. Lett.*, *170*, 433–446.

Tachikawa, K., M. Roy-Barman, A. Michard, D. Thouron, D. Yeghicheyan, and C. Jeandel (2004), Neodymium isotopes in the Mediterranean Sea: Comparison between seawater and sediment signals, *Geochim. Cosmochim. Acta*, *68*, 3095–3106.

Thomas, D. J. (2004), Evidence for deep-water production in the North Pacific Ocean during the early Cenozoic warm interval, *Nature*, *430*, 65–68.

Thomas, D. J., and R. K. Via (2007), Neogene evolution of Atlantic thermohaline circulation: Perspective from Walvis Ridge, southeastern Atlantic Ocean, *Paleoceanography*, *22*, PA2212, doi:10.1029/2006PA001297.

van de Flierdt, T., M. Frank, D.-C. Lee, A. N. Halliday, B. C. Reynolds, and J. R. Hein (2004), New constraints on the sources and behavior of neodymium and hafnium in seawater from Pacific Ocean ferromanganese crusts, *Geochim. Cosmochim. Acta*, *68*, 3827–3843.

van de Flierdt, T., L. F. Robinson, J. F. Adkins, S. R. Hemming, and S. L. Goldstein (2006), Temporal stability of the neodymium isotope signature of the Holocene to glacial North Atlantic, *Paleoceanography*, *21*, PA4102, doi:10.1029/2006PA001294.

Vance, D., and K. Burton (1999), Neodymium isotopes in planktonic foraminifera: A record of the response of continental weathering and ocean circulation rates to climate change, *Earth Planet. Sci. Lett.*, *173*, 365–379.

Vance, D., A. E. Scrivner, P. Beney, M. Staubwasser, G. M. Henderson, and N. C. Slowey (2004), The use of foraminifera as a record of the past neodymium isotope composition of seawater, *Paleoceanography*, *19*, PA2009, doi:10.1029/2003PA000957.

Via, R. K., and D. J. Thomas (2006), Evolution of Atlantic thermohaline circulation: Early Oligocene onset of deep-water production in the North Atlantic, *Geology*, *34*, 441–444, doi:10.1130/G22545.1.

Voelker, A. H. L., S. M. Lebreiro, J. Schonfeld, I. Cacho, H. Erlenkeuser, and F. Abrantes (2006), Mediterranean outflow strengthening during northern hemisphere coolings: A salt source for the glacial Atlantic?, *Earth Planet. Sci. Lett.*, *245*, 39–55.

von Blanckenburg, F., and F. Nägler (2001), Weathering versus circulation-controlled changes in radiogenic isotope tracer composition of the Labrador Sea and North Atlantic Deep Water, *Paleoceanography*, *16*, 424–434.

von Blanckenburg, F., R. K. O'Nions, and J. R. Hein (1996a), Distribution and sources of pre-anthropogenic lead isotopes in deep ocean water from Fe-Mn crusts, *Geochim. Cosmochim. Acta*, *60*, 4957–4963.

von Blanckenburg, F., R. K. O'Nions, N. S. Belshaw, A. Gibb, and J. R. Hein (1996b), Global distribution of beryllium isotopes in deep ocean water as derived from Fe-Mn crusts, *Earth Planet. Sci. Lett.*, *141*, 213–226.

Wright, J. D., and K. G. Miller (1996), Control of North Atlantic Deep Water circulation by the Greenland-Scotland Ridge, *Paleoceanography*, *11*, 157–170.

Zenk, W. (1970), On the temperature and salinity structure of the Mediterranean Water in the northeast Atlantic, *Deep Sea Res.*, *17*, 627–631.